Electrophoretic Mobility Is a Reporter of Hairpin Structure in Single-Stranded DNA Oligomers†

Earle Stellwagen, Arian Abdulla,‡ Qian Dong,§ and Nancy C. Stellwagen*

Department of Biochemistry, University of Iowa, Iowa City, Iowa 52242

Received May 30, 2007; Revised Manuscript Received July 11, 2007

ABSTRACT: The electrophoretic mobilities of 24 single-stranded DNA oligomers, each containing 26 nucleotide residues, have been measured in polyacrylamide gels and in free solution. The mobilities observed at 20 °C differed by ∼20% in polyacrylamide gels and by ∼10% in free solution, even though the oligomers contained the same number of bases. Increasing the temperature or adding urea to the solution equalized the mobilities of the oligomers, suggesting that the variable mobilities observed at 20 °C are due to the formation of stable secondary structures, most likely hairpins. Thermal melting profiles were measured for eight oligomers in 40 mM Tris acetate buffer. The observed melting temperatures of most oligomers correlated roughly with the mobilities observed at 20 °C; however, one oligomer was much more stable than the others. The melting temperatures of four of the oligomers were close to the values predicted by DINAMelt [Markham, N. R., and Zuker, M. (2005) *Nucleic Acids Res. 33,* W577−W581]; melting temperatures of the other oligomers differed significantly from the predicted values. Thermal melting profiles were also measured for two oligomers as a function of the Tris acetate buffer concentration. The salt concentration dependence of the melting temperatures suggests that 0.15 $Tris^+$ ion per phosphate is released upon denaturation. Because the apparent number of $Tris^+$ ions released is greater than that observed by others for the release of Na^+ ions from similar hairpins, the results suggest that DNA hairpins (and, presumably, duplexes) bind more $Tris^+$ ions than Na^+ ions in solution.

Single-stranded DNAs (ssDNA) have been studied for many years because they are essential intermediates in many metabolic processes, including replication, recombination, transcription, and repair. As is well-known, ssDNAs containing inverted repeats have the potential to form stem−loop structures. The designed hairpins most commonly studied contain four or more contiguous Watson−Crick base pairs in the stem and four to six residues in the loop (*1*−*3*). Hairpins with 5−7 base pairs in the stem and 15−30 nucleotides in the loop, called molecular beacons if the ends are fluorescently labeled (*4*−*7*), are also stable and are used extensively as sequence-specific biomolecular probes (*3*, *4*, *8*). At the other size extreme, DNA oligomers with two GC base pairs in the stem and GNA or GNNA residues (where N is any residue) in the loop also form hairpins, some of which are exceptionally stable (*9*, *10*).

The equilibrium between the hairpin (closed) and random coil (open) conformations of a DNA oligomer depends on its sequence and number of residues in the stem and loop (*3*). The loop-closing and stem-closing bases are especially important, because many DNA hairpins are stabilized by noncanonical base pairs closing the loop and stacking on top of the stem, effectively increasing the stem length (*2*, *3*, *9*−*14*). The ionic strength of the solution and the temperature also affect the hairpin−coil equilibrium (*15*−*20*). Kinetic studies have shown that the lifetimes of the open and closed states are ∼100 ms (*21*). Hence, most macroscopic measurements of hairpin-forming DNA oligomers will probe a weighted average of the hairpin and random coil conformations (*6*, *7*, *22*, *23*).

Single-stranded DNA oligomers that do not contain long inverted repeats are usually thought to be random coils in solution. However, as described below, the electrophoretic mobilities of a set of single-stranded oligomers containing 26 nucleotide residues and different A + T contents were highly variable, both in polyacrylamide gels and in free solution, whereas the mobilities of the corresponding double-stranded (ds) DNAs were essentially constant. To investigate whether the variable mobilities observed for the single-stranded oligomers could be due to hairpin formation, the free solution mobilities were measured as a function of temperature and denaturant concentration.

The free solution mobility of a DNA oligomer is a useful probe of hairpin structure (*23*), because the mobility, μ,[1] is

† This work was supported in part by Grant GM061009 from the National Institute of General Medical Sciences (GM061009 to N.C.S). A.A. acknowledges the receipt of a Summer Research Fellowship from the Department of Biochemistry, University of Iowa.

* Corresponding author [telephone (319) 335-7896; fax (319) 335-9570; e-mail nancy-stellwagen@uiowa.edu].

‡ Present address: Department of Biochemistry, Northwestern Oklahoma State University, Alva, OK 73717.

§ Present address: Department of Internal Medicine, University of Iowa, Iowa City, IA 52242.

[1] Abbreviations: CE, capillary electrophoresis; EOF, electroosmotic flow; DINAMelt, structure prediction algorithm; mu, mobility units, 1 mu = 1 × 10^{-4} cm^2/Vs; μ, mobility; $\Delta\mu_{diff}$, span of the mobility transition; T_m, melting temperature.

10.1021/bi701058f CCC: $37.00
Published on Web 09/01/2007

Table 1: Sequences of the Forward Strands of the Single-Stranded Oligomers in the Variable %AT Family

oligomer name[a]	sequence
38f	CGCAAAATCGGGCAAAATCGGCGGCG
42f	CGCAAAATCGGGCAAAATCGCTGGCG
46f	CGCAAAATCGGTCAAAATCGGCTGCG
50f	CGCAAAATCTGTCAAAATCGCTGGCG
54f	CGCAAAATCTGTCAAAATCTGCGTCG
58f	CGCAAAATCTGTCAAAATCTGTCTCG
62f	CGTAAAATCTGTCAAAATCTGTCTCG
65f	CGTAAAATCTGTCAAAATCTATCTCG
69f	CGTAAAATCTGTCAAAATCTATTACG
73f	CGTAAAATCTATCAAAATCTATTACG
77f	CGTAAAATATATCAAAATCTATTACG
81f	CGTAAAATATATCAAAATATATTACG

[a] The A + T content in each sequence is indicated by the name.

determined by the ratio between the effective charge of the analyte, *Q*, and its frictional coefficient, *f*, as shown in eq 1 (*24*):

$$\mu = Q/f \quad (1)$$

Single-stranded oligomers containing the same number of nucleotides would be expected to have the same effective charge under a given set of experimental conditions, in the absence of sequence-specific cation binding. However, hairpins are more compact than random coils and, therefore, would be expected to have smaller frictional coefficients and exhibit larger electrophoretic mobilities than random coils containing the same number of nucleotides. In agreement with this expectation, DNA minihairpins containing eight nucleotide residues have been shown to exhibit higher electrophoretic mobilities than the random coil forms of the same oligomers (*23*). The mobilities of the minihairpins decreased toward a common value with increasing temperature or denaturant concentration, as the random coil conformation of each oligomer became dominant (*23*).

Here, hairpin formation has been investigated in a set of single-stranded DNA oligomers containing 26 nucleotide residues, using capillary electrophoresis (CE) to measure the free solution mobility. Increasing the temperature or adding 7 M urea to the solution equalized the mobilities, indicating that the variable mobilities observed in buffer solutions at 20 °C are due to the presence of relatively compact secondary structures, most likely hairpins. Detailed thermal melting studies were carried out with eight oligomers. The melting temperatures were roughly correlated with the mobilities observed at 20 °C; however, one oligomer was exceptionally stable and melted at a much higher temperature. The salt concentration dependence of the melting temperatures suggests that the number of $Tris^+$ ions released by DNA hairpins upon denaturation is greater than predicted (*25*) and observed (*19*) for the release of Na^+ ions by DNA hairpins of similar size and base pair composition. The implications of the results are discussed.

MATERIALS AND METHODS

DNA Samples. The DNA oligomers used in this study contained 26 bases or base pairs, two phased AAAAT or TTTTA sequence motifs, and CG residues at each end. The remaining nucleotides were varied to give total A + T contents ranging from 38 to 81%. The sequences of the forward strands of the oligomers studied in this work are listed in Table 1; the corresponding reverse sequences and duplexes were also characterized. For brevity, the forward strands in Table 1 are denoted 38f to 81f, to indicate the percent A + T in each oligomer; the reverse strands are denoted 38r to 81r. Collectively, the single-stranded oligomers are described as the variable %AT family. Plasmid pUC19, linearized by the blunt-cutting restriction enzyme *Ssp*I, was used as a marker in the initial CE experiments. An oligomer containing five nucleotides, with the sequence ACCGC (denoted ss5), was used as the marker in the thermal denaturation studies. The oligomers were synthesized by Integrated DNA Technologies (IDT, Coralville, IA) and purified by HPLC or polyacrylamide gel electrophoresis. They migrated as single bands in polyacrylamide gels and exhibited single peaks when characterized by CE. All oligomers were dissolved in 10 mM Tris−Cl buffer, pH 8.0, and stored at −20 °C until needed. Duplexes were prepared

by heating equimolar mixtures of complementary single strands to 95 °C in the same buffer and slowly cooling to ambient temperature. All duplexes were monodisperse and gave rise to single bands in polyacrylamide gels and single peaks in the CE electropherograms.

Polyacrylamide Gel Electrophoresis. The various single- and double-stranded oligomers were electrophoresed in polyacrylamide gels containing 9.3% T (w/v total acrylamide plus Bis[*N*,*N*′-methylenebisacrylamide] crosslinker) and 3% C (w/w % Bis in % T), using methods described previously (*26*). The gels were cast and run in 40 mM Tris acetate−EDTA buffer (0.04 M Tris base, brought to pH 8.0 with glacial acetic acid, plus 1 mM EDTA). All gels were aged overnight in a refrigerator and pre-electrophoresed for 1 h to eliminate charged impurities remaining after polymerization (*26*). The temperature in the gel during electrophoresis, measured by inserting a thermister into each gel after each run, was 6 ± 1 °C. The 10- and 50-bp DNA ladders (Invitrogen) were used as gel mobility markers.

Capillary Electrophoresis. Capillary zone electrophoresis measurements were carried out using a Beckman Coulter P/ACE MDQ Capillary Electrophoresis System (Fullerton CA), run in the reverse polarity mode (anode on the detector side) with UV detection at 254 nm, as described previously (*27*, *28*). LPA capillaries (Bio-Rad, Hercules, CA) coated with linear polyacrylamide were used to minimize the electroosmotic flow (EOF) of the solvent. Previous studies have shown that polyacrylamide coatings do not alter the free solution mobilities (*29*). The capillaries had external diameters of 375 μm and internal diameters of 75 μm and were typically 39.3 cm in length (29.0 cm to the detector). The capillary cartridge was thermostated at temperatures ranging from 15 to 60 °C, the range available with the instrument. The samples were hydrodynamically injected into the capillary by applying a pressure of 0.5 psi (0.0035 MPa) for 3 s. The injection volume was 22.5 nL; the sample plug occupied 1.3% of capillary length. The electric field ranged between 60 and 425 V/cm; however, the current in the capillary was always kept below 30 μA to minimize Joule heating. Control experiments have shown that the DNA mobilities measured under these conditions are independent of DNA concentration, the length of the sample plug, and the electric field strength (*27*, *29*).

CE measurements at 20 °C were carried out using either 20 mM sodium diethylmalonate buffer, pH 7.3, or 40 mM Tris acetate buffer, pH 8.2, as the background electrolyte. Similar results were observed in both buffers; therefore, detailed thermal denaturation studies were carried out only in 40 mM Tris acetate buffer. For two oligomers, 77f and 77r, thermal denaturation experiments were carried out in Tris acetate buffers varying in concentration from 40 to 240 mM. Because the pH of the Tris acetate buffers was equal to the pK_a of Tris base, the concentration of $Tris^+$ ions in the various solutions ranged from 20 to 120 mM. To avoid confusion in the following discussion, all buffers are described in terms of both the total concentration of the buffering ion (the usual practice) and the concentration of the cation present in the solution.

The thermal dependence of the pK_a of Tris buffers does not affect the melting studies, for two reasons. First, we found that Tris acetate buffers ranging from 40 to 240 mM in concentration have a $\Delta pH/\Delta T$ of -0.028 ± 0.002 over the temperature range from 15 to 60 °C. The observed $\Delta pH/\Delta T$ value is exactly equal to the published $\Delta pK_a/\Delta T$ value, −0.028 (*30*). Thus, although the pH of the Tris acetate buffer decreased with increasing temperature, the ionic strength of the buffer remained constant because the pK_a of the buffer decreased in parallel. Second, DNA has no ionizable groups in the pH range of the Tris buffers, from pH 8.35 to pH 7.10, between 15 and 60 °C.

Correction of the Observed Mobilities to Constant Temperature. The free solution mobilities of the various oligomers were calculated from the observed migration times, using eq 2

$$\mu_{oligo}^{obsd} = L_d/Et \tag{2}$$

where μ_{oligo}^{obsd} is the observed mobility of the oligomer, L_d is the distance to the detector (in cm), E is the electric field strength (in V/cm), and t is the time required for the sample to migrate to the detector (in s). The observed mobility is the algebraic sum of the actual mobility of the oligomer and the mobility due to the electroosmotic flow (EOF) of the solvent, μ_{EOF}, as shown in eq 3

$$\mu_{oligo}^{corr} = \mu_{oligo}^{obsd} + \mu_{EOF} \tag{3}$$

where μ_{oligo}^{corr} is the EOF-corrected mobility of the oligomer (*29*, *31*). A similar equation can be written for the marker. If the mobilities of the oligomer and the marker are measured in the same solution at the same time, μ_{EOF} will be the same for both samples, and the difference in mobility between the oligomer and the marker, $\Delta\mu$

$$\Delta\mu = \mu_{oligo}^{obsd} - \mu_{mark}^{obsd} = \mu_{oligo}^{corr} - \mu_{mark}^{corr} \tag{4}$$

will be independent of the EOF. Upon rearranging, the EOF-corrected mobility of the oligomer is given by eq 5:

$$\mu_{oligo}^{corr} = \mu_{mark}^{corr} + \Delta\mu \tag{5}$$

For measurements in sodium diethylmalonate buffer, the marker was linear pUC19, and μ_{mark}^{corr} was taken to be 3.21 mu (mobility units; 1 mu = 1×10^{-4} cm^2/Vs) at 20 °C, the average mobility observed in 24 independent measurements. For the thermal melting studies in Tris acetate buffers, the marker was ss5. To make the EOF correction at different temperatures, the mobility of ss5 was first measured as a function of temperature and buffer concentration, with the results shown in Figure 1. Because the mobility increased linearly with increasing temperature (see below), the equations of the lines were taken to be the expected mobility of the marker at the given temperature and buffer concentration. Any deviation of the observed mobility of the marker from the expected value was assumed to be due to μ_{EOF}, which was then used to correct the observed mobility according to eq 3. The EOF-corrected mobilities of the various oligomers were typically constant within ±0.01 mu, regardless of the type of buffer, the marker used in the experiment, or whether the measurements were repeated on the same day or on different days.

The linear increase of the mobility of ss5 (and the oligomers) with increasing temperature (Figure 1) is due to the fact that $\mu_{obsd} \sim \epsilon/\eta$, where ϵ is the dielectric constant

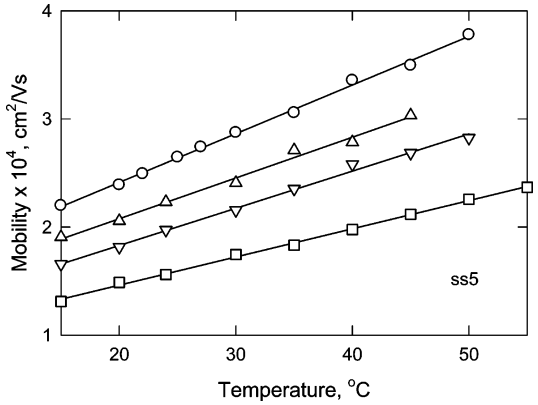

FIGURE 1: Dependence of the observed mobility of the marker, ss5, on temperature in (○) 40 mM Tris acetate buffer (20 mM Tris$^+$), (▽) 80 mM Tris acetate buffer (40 mM Tris$^+$), (△) 120 mM Tris acetate buffer (60 mM Tris$^+$), and (□) 240 mM Tris acetate buffer (120 mM Tris$^+$). The lines were drawn by linear regression.

and η the viscosity of the solvent (*23*, *32*−*36*). The large differences in mobility due to changes in the physical properties of the solvent with temperature (Figure 1) would obscure smaller mobility differences due to hairpin−random coil transitions (*23*). Therefore, the mobilities of the oligomers must first be corrected to constant temperature conditions (here 20 °C). Different methods of making this correction have been described previously (*23*). One of the easiest and most accurate methods is to calculate the ratio of the EOF-corrected mobilities of the test oligomer and a marker at various temperatures and multiply the mobility ratio by the corrected mobility of the marker at 20 °C, $\mu_{mark}^{corr,20}$, as shown in eq 6

$$\mu_{oligo}^{corr,20} = \mu_{mark}^{corr,20}\left(\frac{\mu_{oligo}^{corr,T}}{\mu_{mark}^{corr,T}}\right) = \mu_{mark}^{corr,20}\left(\frac{\mu_{oligo}^{obsd,T} + \mu_{EOF,T}}{\mu_{mark}^{obsd,T} + \mu_{EOF,T}}\right) \quad (6)$$

where the symbol *T* indicates that the mobility was measured at temperature *T*. The second equality in eq 6 explicitly includes the EOF correction to the observed mobilities. The superscript 20 has been added to the symbol for the EOF-corrected mobility of the oligomer to indicate that it is the mobility that would have been observed if the solvent had had the properties of water at 20 °C. For simplicity, the values of $\mu_{oligo}^{corr,20}$ for the various oligomers are called the temperature-corrected mobilities in the subsequent text. It is important that the marker not undergo a structural transition over the investigated temperature range. In the present case, ss5 is too short to form a hairpin and, therefore, is a suitable marker for the thermal denaturation experiments.

The temperature-corrected mobilities of the various oligomers were plotted as a function of temperature and analyzed by a four-parameter Hill equation, using SigmaPlot, to calculate the limiting mobilities of the hairpin and coil forms of each oligomer and the midpoint of the melting transition. Unless otherwise indicated, all parameters were allowed to vary independently during the calculation.

RESULTS AND DISCUSSION

Characterization of Single-Stranded Oligomers by Polyacrylamide Gel Electrophoresis. A photograph of a typical

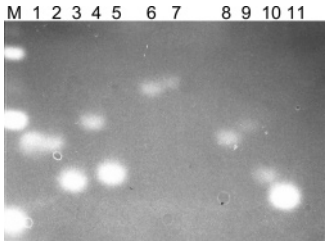

FIGURE 2: Typical electropherogram observed for 11 members of the variable %AT family in a polyacrylamide gel containing 9.3% T and 3% C. Lanes 1−11 contain oligomers 38f, 42f, 46f, 50f, 54f, 58f, 62f, 69f, 73f, 77f, and 81f, respectively; lane M contains the 10-bp ladder, with the 30, 20, and 10 bp fragments visible (from top to bottom). The gel was cast and run in 40 mM Tris acetate−EDTA buffer at 6 °C.

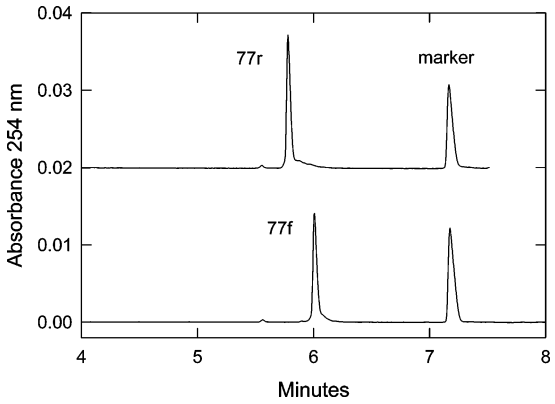

FIGURE 3: Electropherograms observed by capillary electrophoresis for oligomers 77f and 77r in 40 mM Tris acetate buffer (20 mM Tris$^+$) at 15 °C. The peaks on the left correspond to 77r (top) and 77f (bottom); the peaks on the right correspond to the marker, ss5.

electropherogram observed for 11 members of the variable %AT family in a 9.3% T, 3% C polyacrylamide gel is shown in Figure 2. The left-most lane (M) contains the 10-bp DNA ladder, with the 30-, 20-, and 10-bp fragments visible (from top to bottom). Lanes marked 1−11 contain oligomers 38f, 42f, 46f, 50f, 54f, 58f, 62f, 69f, 73f, 77f, and 81f, respectively. The apparent absolute mobilities observed for the 24 single-stranded members of the variable %AT family ranged from 0.67 to 0.80 mu, with an average value of 0.74 ± 0.05 mu. By contrast, the corresponding duplexes exhibited nearly constant apparent absolute mobilities in polyacrylamide gels, with an average value of 0.65 ± 0.01 mu (data not shown).

Free Solution Mobilities of the Variable %AT Family. To eliminate the possible influence of the polyacrylamide gel matrix on the mobilities observed for the single-stranded oligomers in the variable %AT family, the mobilities were measured in free solution by capillary electrophoresis. Typical electropherograms observed for oligomers 77f and 77r at 15 °C are illustrated in Figure 3. Similar electropherograms were observed for the other oligomers (not shown).

The mobilities observed for the single- and double-stranded members of the variable %AT family, measured in sodium diethylmalonate buffer at 20 °C, are illustrated in Figure 4. The mobilities of the double-stranded oligomers were nearly independent of base pair composition, with an average value of 3.38 ± 0.01 mu. These small mobility differences will be discussed in a future publication. By contrast, the mobilities of the various single-stranded oligomers ranged from 3.10 to 3.39 mu, with an average value of

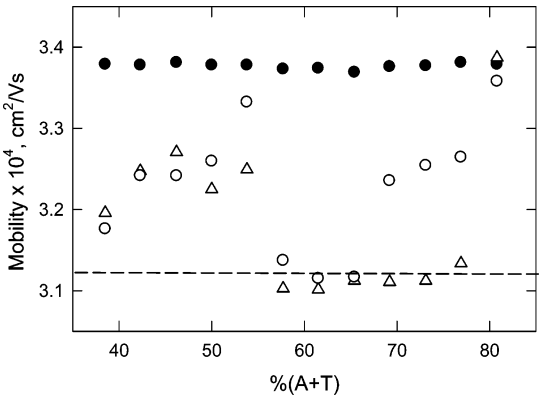

FIGURE 4: Free solution mobilities observed at 20 °C for the single- and double-stranded members of the variable %AT family, plotted as a function of the percent A + T in each oligomer: (●) duplex DNAs; (△) forward strands of oligomers listed in Table 1; (○) reverse strands. The dashed line corresponds to the average mobility observed for oligomers in the slow mobility group. The background electrolyte was 20 mM sodium diethylmalonate buffer (30 mM Na^+).

3.21 ± 0.09 mu. There is no correlation between the free solution mobility and the A + T content of the oligomer.

The mobilities observed for the single-stranded oligomers in Figure 4 fall into two groups. Nine oligomers exhibited approximately constant, relatively slow mobilities with an average value of 3.12 ± 0.01 mu, as indicated by the dashed line in the figure. The other 15 oligomers exhibited larger, highly variable mobilities, with an average value of 3.21 ± 0.06 mu. Interestingly, the forward strands of oligomers containing 69, 73, and 77% A + T fell in the slow group, whereas the reverse strands exhibited significantly higher mobilities.

Studies with model DNA minihairpins in free solution have shown that hairpins migrate more quickly than random coils containing the same number of nucleotides (*23*). Therefore, it seems reasonable to assume that oligomers with mobilities in the slow group in Figure 4 are primarily in the random coil conformation, whereas oligomers with faster mobilities are likely to contain some hairpin structure. Because hairpins and random coils are in fast exchange (*21*−*23*), the mobility observed for an oligomer containing significant populations of both conformational isomers will be the weighted average of the mobilities of each of the conformers, as shown by eq 7

$$\mu_{obs} = N_h \cdot \mu_{hairpin} + N_c \cdot \mu_{coil} \quad (7)$$

where N_h and N_r are the mole fractions of hairpin and random coils present in the solution and $N_h + N_c = 1$.

To verify that hairpin formation was responsible for the different mobilities observed for the single-stranded oligomers in the variable %AT family, the mobilities of oligomers 77f (slow mobility group) and 77r (faster mobility) were measured both as a function of temperature and, at 20 °C, in buffers containing various quantities of urea. Because the A + T contents of the two strands are identical, their mobilities would be expected to converge to the same value at high temperatures or high denaturant concentrations, if the higher mobility of 77r was due to hairpin formation. The results are shown in Figure 5, where the mobility ratio, μ_{77r}/μ_{77f}, is plotted as a function of temperature (panel A) or urea

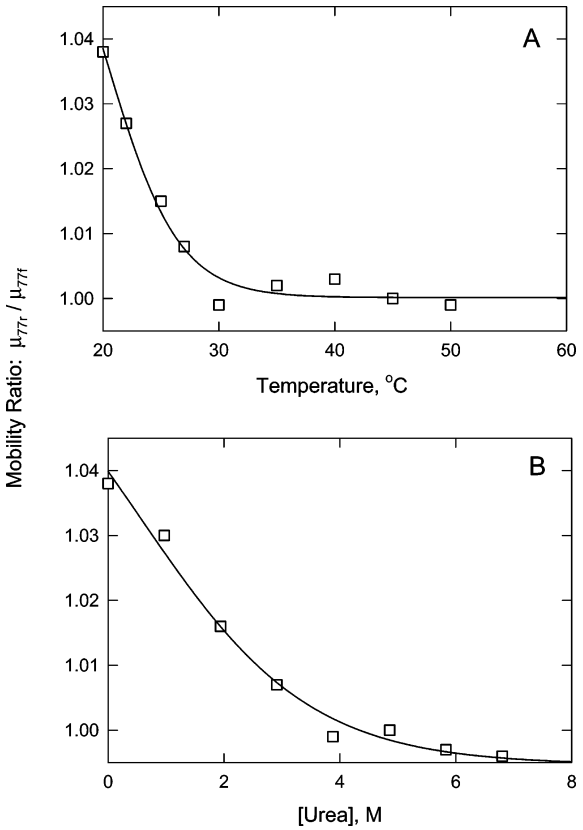

FIGURE 5: Mobility ratios, μ_{77r}/μ_{77f}, plotted as a function of (A) temperature and (B) urea concentration. In both cases, the background electrolyte was 40 mM Tris acetate buffer (20 mM $Tris^+$). The temperature was 20 °C in panel B.

concentration (panel B). The mobility ratio decreased from its initial value of 1.04 to a limiting plateau value of 1.00 with increasing temperature or denaturant concentration, respectively. Hence, oligomer 77r contains a population of relatively compact secondary structures that can be unfolded by heat or chemical denaturants. These secondary structures are assumed to be hairpins by analogy with the hairpin structures predicted for the same oligomers by the structure prediction algorithm MFOLD (*15*) or its updated version, DINAMelt (*16*, *25*, *37*). The predicted hairpin structures are discussed below.

To establish the generality of these results, detailed thermal melting studies were carried out using four pairs of oligomers in the %AT family. The chosen oligomers contained 81% A + T (fastest observed mobilities), 62% A + T (slow mobility group), 42% A + T (intermediate mobilities), and 77% A + T (forward strand with slow mobility; reverse strand with intermediate mobility). The mobilities observed for each of the oligomers in 40 mM Tris acetate buffer (20 mM $Tris^+$) at 20 °C are given in the seventh column of Table 2. All thermal transitions were reversible; the mobilities of the various oligomers (and the marker) at low temperatures were always recovered after the solution was heated above the melting temperature. The widths of the peaks in the electropherograms were also independent of temperature, indicating that fast exchange between conformational isomers was occurring at all temperatures.

Thermal Melting Transitions Observed for Single-Stranded Oligomers Containing 81% A + T. The temperature-corrected mobilities observed for oligomers 81f and 81r

Table 2: Mobilities and Melting Temperatures Measured for Oligomers in 40 mM Tris Acetate Buffer (20 mM $Tris^+$) and Comparison with the Predicted (*25*) Melting Temperatures in 20 mM Na^+

oligomer	$\mu_{hairpin}$,[a] mu	μ_{coil},[a] mu	$\Delta\mu_{diff}$,[a] mu	obsd T_m,[b] °C	predicted T_m,[c] °C	$\mu_{obs,20°}$,[a] mu	% hairpin
81f	3.06	2.84	0.22	33	37	3.06	100
81r	3.07	2.84	0.22	33	38	3.07	100
77f	2.88	2.84	0.17[d]	5	31	2.88	23
77r	2.98	2.84	0.17	24	29	2.98	82
62f	2.84	2.84	0.14[e]	−2	19	2.84	0
62r	2.89	2.84	0.14[e]	−2	38	2.89	35
42f	2.96	2.84[f]	0.14	52	32	2.96	86
42r	2.95	2.85	0.14[e]	35	34[g]	2.95	71

[a] Mobility units, 1 mu = 10^{-4} cm^2/Vs. [b] Measured in solutions containing 20 mM $Tris^+$. [c] Predicted by DINAMelt (*25*) for solutions containing 20 mM Na^+. [d] Held constant to the value observed for 77r. [e] Held constant to the value observed for 42f. [f] Set equal to μ_{coil} of 81f and 81r. [g] Average melting temperature of the three most stable predicted hairpin structures.

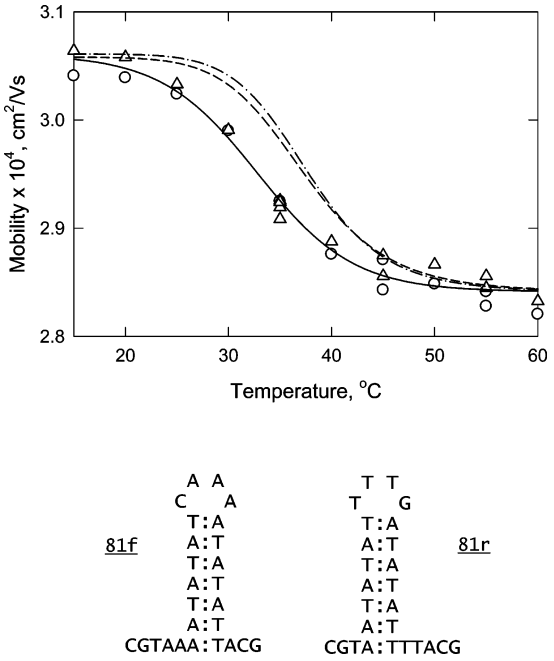

FIGURE 6: Dependence of the temperature-corrected mobilities of oligomers 81f (△) and 81r (○) on temperature. The background electrolyte was 40 mM Tris acetate buffer (20 mM $Tris^+$). The solid line was calculated with the fitting parameters given in Table 2; the dashed and dot-dashed lines correspond to the melting curves predicted for 81f and 81r, respectively, from the free energies given in DINAMelt (*25*). The most stable predicted (*25*) hairpin structures of the two oligomers are illustrated at the bottom of the figure.

(fastest observed mobilities at 20 °C) are plotted as a function of temperature in Figure 6. Very similar melting curves were observed for the two oligomers; therefore, the two data sets were fit to a common transition. The midpoint of the melting transition, called the melting temperature, T_m, for brevity, was 33 °C. The limiting temperature-corrected mobilities of the hairpin and coil conformations were 3.06 and 2.84 mu, respectively. Hence, the mobility difference between the two conformations, $\Delta\mu_{diff}$, was 0.22 mu. This fitting parameter will be called the span of the transition in the subsequent text. The solid line in Figure 6 was calculated with these fitting parameters; for reference, these values are also given in columns 2−5 of Table 2.

Thermal melting curves can also be predicted for oligomers 81f and 81r from the structure prediction algorithm DINAMelt (*16*, *25*, *37*). This program predicts the most likely structure(s) of the hairpin(s) populated by a given sequence at a given temperature and salt concentration and estimates the melting temperature(s) and the free energy (ΔG) of the melting transition(s). The program is based on thermal melting studies of DNA oligomers carried out in solutions containing sodium as the counterion (*16*). Unpublished experiments cited in refs *15* and *38* have indicated that K^+ and NH_4^+ ions have the same effect on DNA melting as Na^+ ions, suggesting that all monovalent cations are equivalent in this respect. The validity of this assumption will be discussed below.

The ΔG values predicted by DINAMelt at different temperatures can be used to estimate the fractional population of hairpins present at each temperature, assuming that the hairpin−coil equilibrium is a two-state reaction, because $-\Delta G = RT \ln K_{eq}$ (where R is the gas constant, T is the absolute temperature, and K_{eq} is the hairpin/random coil equilibrium constant). Equation 7 can then be used to predict the mobility of the oligomer as a function of temperature, if the temperature-corrected mobilities of the hairpin and coil structures are known or can be estimated (*23*). For oligomers with 81% A + T, the hairpin and coil mobilities were assumed to be the limiting mobilities calculated from the experimental data by curve fitting (Table 2). These values were used to calculated the dashed and dot-dashed curves in Figure 6. The melting temperatures predicted (*25*) for oligomers 81f and 81r are 37 and 38 °C, respectively, somewhat higher than the observed melting temperature of 33 °C. For convenience, the measured and predicted T_m values are compared in columns 5 and 6 of Table 2.

The most stable hairpin structures predicted by DINAMelt (*25*) for oligomers 81f and 81r have 7 contiguous A−T base pairs in the stem and four unpaired residues in the loop, as shown in the lower portion of Figure 6. Hairpins with YTTR sequences (as predicted for 81r) are known to be stabilized by base pairing between the loop-closing Y and R residues, leaving only two unpaired T residues at the tip of the loop (*1*, *3*). Loops containing the YAAR sequence motif appear to be equally stable, because the thermal melting transitions of 81f and 81r are nearly identical.

Thermal Melting Transitions of Single-Stranded Oligomers Containing 42% A + T. The thermal melting profiles observed for oligomers 42f and 42r (intermediate mobilities at 20 °C) are illustrated in Figure 7. For 42f (panel A), the temperature-corrected mobilities were essentially constant between 15 and 30 °C, defining the limiting mobility of the hairpin form of this oligomer (2.98 mu). The plateau value of the mobility at high temperatures could not be reached during the experiment because of instrumental limitations. However, it is reasonable to assume that the random coil form of this oligomer would have the same limiting mobility as observed for oligomers 81f, 81r, and 42r (see below) at high temperatures (2.84 mu), making the span of the transition 0.14 mu. Holding $\Delta\mu_{diff}$ constant at this value, the melting temperature and the limiting mobilities of the hairpin and random coil forms of 42f were calculated by curve fitting. The melting temperature calculated for this oligomer, 52 °C, is much higher than those observed for 81f and 81r, which explains why only a portion of the melting transition

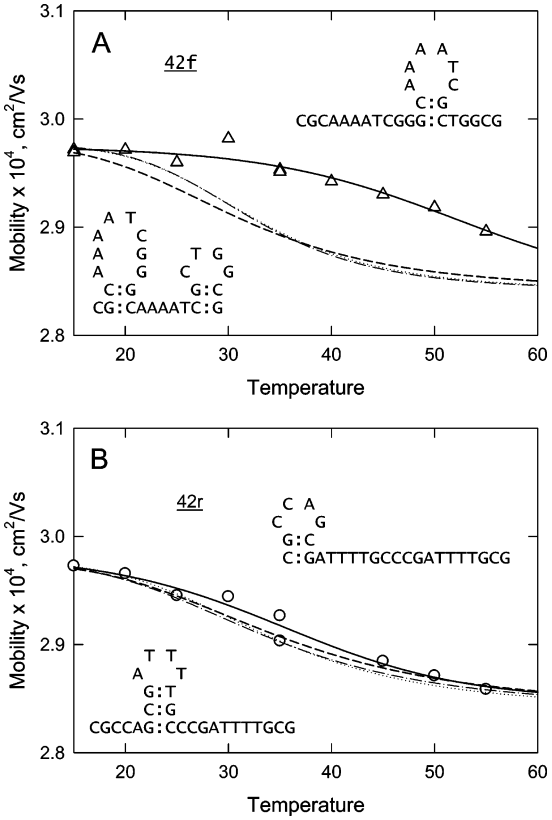

FIGURE 7: Thermal melting curves observed for oligomers containing 42% A + T, measured in 40 mM Tris acetate buffer (20 mM $Tris^+$): (A) 42f; (B) 42r. In both panels A and B, the symbols correspond to the temperature-corrected mobilities and the solid lines are drawn with the fitting parameters given in Table 2. Two of the most stable predicted (*25*) structures for 42f and 42r are shown as insets in panels A and B, respectively. The dashed, dot-dashed, and dotted lines correspond to the predicted melting curves of these hairpins.

could be observed in the available temperature window. The various fitting parameters are summarized in Table 2; the solid line in Figure 7A was calculated with these parameters.

For oligomer 42r (panel B), the temperature-corrected mobility at 15 °C equaled that of 42f (2.98 mu), suggesting that the hairpin forms of the two oligomers have the same limiting mobility. The mobility of 42r at high temperatures agreed with those observed for 81f and 81r (2.84 mu). Therefore, the span of the transition was assumed to be 0.14 mu, and the melting temperature and the limiting hairpin and coil mobilities were calculated from the mobility data by curve fitting. The melting temperature of oligomer 42r was found to be 35 °C, much lower than that observed for 42f, even though both oligomers had similar mobilities at 20 °C (Figure 4 and Table 2). The solid line in Figure 7B was calculated with these fitting parameters; they are also summarized in Table 2.

The melting curves predicted for oligomers 42f and 42r from the DINAMelt (*25*) free energies of the most stable hairpin forms of each oligomer are shown as the dashed, dot-dashed, and dotted curves in Figures 7A,B. For 42f (panel A), the predicted melting curves are very different from the observed melting curve. The predicted melting temperatures of the two most stable hairpin forms of this oligomer (insets in panel A) are 32 °C, much lower than the observed melting temperature of 52 °C. For 42r (panel B), the predicted

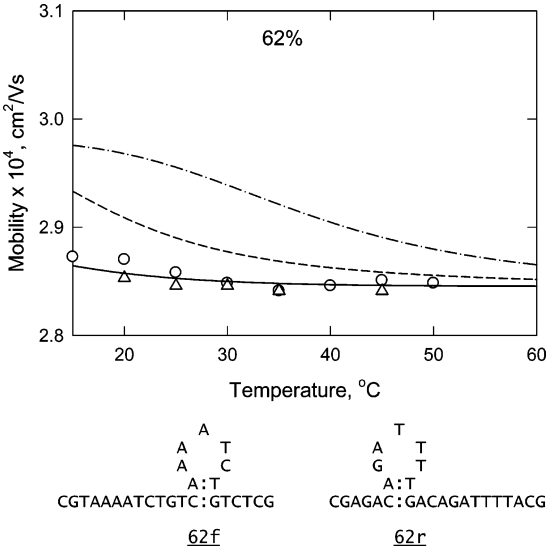

FIGURE 8: (A) Thermal melting transitions observed for oligomers containing 62% A + T, measured in 40 mM Tris acetate buffer (20 mM $Tris^+$). The symbols correspond to the temperature-corrected mobilities of (△) 62f and (○) 62r. The solid line was calculated using the fitting parameters given in Table 2. The dashed and dot-dashed lines correspond to the predicted (*25*) melting curves of 62f and 62r, respectively. The most stable predicted hairpin structures of 62f and 62r are shown in the lower portion of the figure.

melting curves are very similar to the experimental curve; the predicted melting temperatures range from 33 to 35 °C for the three most stable hairpin forms of this oligomer. The structures of two of the three most stable predicted hairpins are shown as insets in panel B.

It is not clear why oligomer 42f is so much more stable than 42r and why the melting temperature of 42f is poorly predicted by DINAMelt. However, one of the predicted 42f structures contains a CTGG loop with a GC base pair closing the top of the stem. SELEX selection experiments have identified this sequence motif as an exceptionally stable DNA tetraloop (*2*). Previous studies have shown that the melting temperatures of unusually stable DNA hairpins are not well predicted by MFOLD (*23*).

Thermal Melting Transitions of Single-Stranded Oligomers Containing 62% A + T. The temperature-corrected mobilities of oligomers 62f and 62r (slow mobility group) decrease only slowly with increasing temperature, as shown in Figure 8, because only the tails of the melting transitions are observed in the available temperature window. The plateau mobilities observed for the two oligomers at high temperatures, 2.84 mu, are equal to the mobilities observed for the random coil forms of 81f, 81r, and 42r. However, the mobilities of the hairpin forms of 62f and 62r are uncertain. Each oligomer is predicted (*25*) to form a hairpin with a two base pair CA/TG stem and a five residue loop, as shown in the lower portion of Figure 8. The hairpin loops are similar in size to the hairpin loops predicted for 42f and 42r. Hence, it seems reasonable to assume that the hairpin forms of 62f and 62r would have mobilities similar to the mobilities of the hairpin forms of 42f and 42r and that the span of the transition would be the same, 0.14 mu. The melting curve shown by the solid line in Figure 8 was calculated with these assumptions; it appears to fit the data reasonably well. The fitting parameters are given in Table 2; the calculated melting temperature is −2 °C.

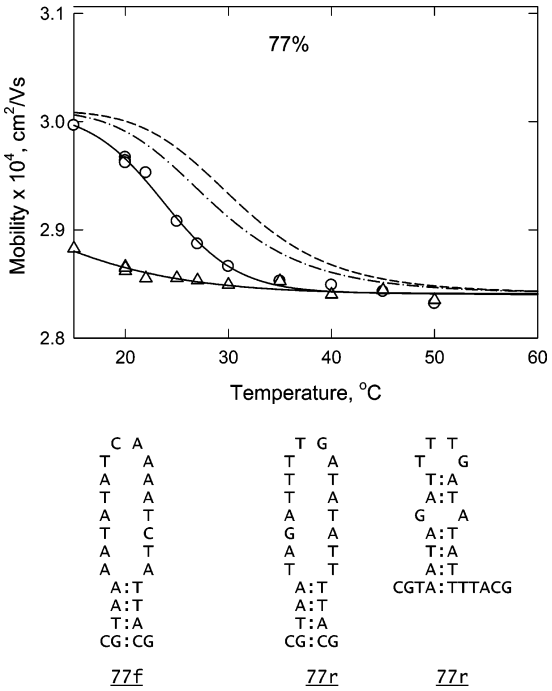

FIGURE 9: Thermal melting curves observed for oligomers containing 77% A + T, measured in 40 mM Tris acetate buffer (20 mM $Tris^+$). The symbols correspond to the temperature-corrected mobilities of (△) 77f and (○) 77r. The solid lines were calculated using the fitting parameters given in Table 2. The dashed (77f) and dot-dashed (77r) lines correspond to the predicted melting curves. The lower portion of the figure illustrates the most stable predicted (*25*) hairpin structures of 77f (left) and 77r (middle). A less stable hairpin structure of 77r is illustrated at the bottom right. The T_m of this hairpin is predicted (*25*) to be 22 °C.

The melting curves predicted for oligomers 62f and 62r from the DINAMelt free energies (*25*) are shown as the dashed and dot-dashed curves in Figure 8. The predicted melting temperatures are 19 and 38 °C for 62f and 62r, respectively, much higher than the T_m values determined experimentally.

Thermal Melting Transitions of Single-Stranded Oligomers Containing 77% A + T. The temperature-corrected mobilities of oligomers 77f (slow mobility group) and 77r (intermediate mobility) are plotted as a function of temperature in Figure 9. As expected from the results in Figure 5, 77r exhibits a distinct melting transition in Tris acetate buffer, whereas only the tail of the melting transition is observed for 77f. The mobilities observed for the two oligomers at high temperature are equal to the values observed for the other oligomers at high temperatures (2.84 mu), indicating that the mobilities of the random coil forms of all members of the variable %AT family are equal. The melting curve of 77r was analyzed by allowing all three fitting parameters (limiting mobilities of the hairpin and random coil conformations and the melting temperature) to vary independently. The limiting mobility of the hairpin form of 77f, which cannot be determined from Figure 9, was assumed to be equal to that of 77r, so that the span of the transition would be the same for both oligomers. The melting temperatures calculated for 77f and 77r were found to be 5 and 24 °C, respectively. The melting temperatures and limiting mobilities of the hairpin and coil structures are given in Table 2; the solid lines in Figure 9 were calculated with these fitting parameters.

The predicted (*25*) hairpin structures of 77f and 77r are illustrated in the lower portion of Figure 8. The most stable hairpins of both oligomers have 4 Watson−Crick base pairs in the stem (5, if the terminal C and G residues form a base pair) and large loops containing 16 residues. These predicted structures are similar to those of molecular beacons, which typically have 5−7 residues in the stem and 15−30 residues in the loop (*4*, *5*, *8*). The thermal transitions predicted for these two hairpins from the DINAMelt free energies (*25*) are shown as the dashed and dot-dashed curves in Figure 8; the melting temperatures predicted for 77f and 77r are 31 and 29 °C, respectively. The predicted melting temperature of 77r is similar to the observed T_m of 25 °C; however, the predicted T_m of 77f is much higher than the observed value (5 °C).

The similarity of the most stable predicted hairpin structures of oligomers 77f and 77r does not explain the large differences in their melting temperatures. However, oligomer 77r is predicted to form a second, less stable hairpin with a four-residue loop and six Watson−Crick base pairs flanking a (possibly) sheared GA base pair in the stem, as shown by the right-most structure at the bottom of Figure 9. The predicted melting temperature of this hairpin is 22 °C, close to the observed T_m of 24 °C. The TTTG loop in this hairpin fits the YTTR pattern, which is known to form exceptionally stable tetraloops (*1*, *2*). Hence, the conformational ensemble of oligomer 77r may include a significant population of this hairpin structure. If both hairpin structures were populated, their individual melting transitions would not be observed because the transitions are broad and have similar midpoints.

Salt Dependence of Thermal Melting Temperatures of Oligomers Containing 77% A + T. The mobilities of oligomers 77r and 77f were also measured as a function of temperature in 80, 120, and 240 mM Tris acetate buffer (40, 60, and 120 mM $Tris^+$ ions). The temperature-corrected mobilities of both oligomers decreased progressively with increasing buffer concentration, as shown in Figure 10, because of the increased electrostatic shielding of the charged phosphate residues with increasing ionic strength (*32*, *39*). Analysis of the thermal transitions using the methods described in the previous section indicates that the melting temperature of 77r increased from 24 to 36 °C as [$Tris^+$] increased from 20 to 120 mM; the melting temperature of 77f increased from 5 to 22 °C over the same range. The increased melting temperatures observed at high [$Tris^+$] caused the thermal transitions to become better defined, especially for 77f (panel B), because more of the transition was shifted into the observable temperature window.

The melting curves predicted for the most stable hairpin forms of 77f and 77r (left two structures at the bottom of Figure 9) are shown as the dashed lines in Figure 10. For 77r (panel A), the predicted and measured melting curves agree when the $Tris^+$ concentration is 120 mM; the experimental curve is not shown for clarity. However, the predicted and measured melting curves diverge progressively as the $Tris^+$ concentration is decreased, suggesting that Na^+ and $Tris^+$ ions have different effects on hairpin stability, especially at low ionic strengths. The predicted and measured melting curves for 77f are significantly different at all [$Tris^+$], as shown for the two extremes, 20 and 120 mM $Tris^+$, in panel B. The measured and predicted melting temperatures of the two oligomers are summarized in Table 3.

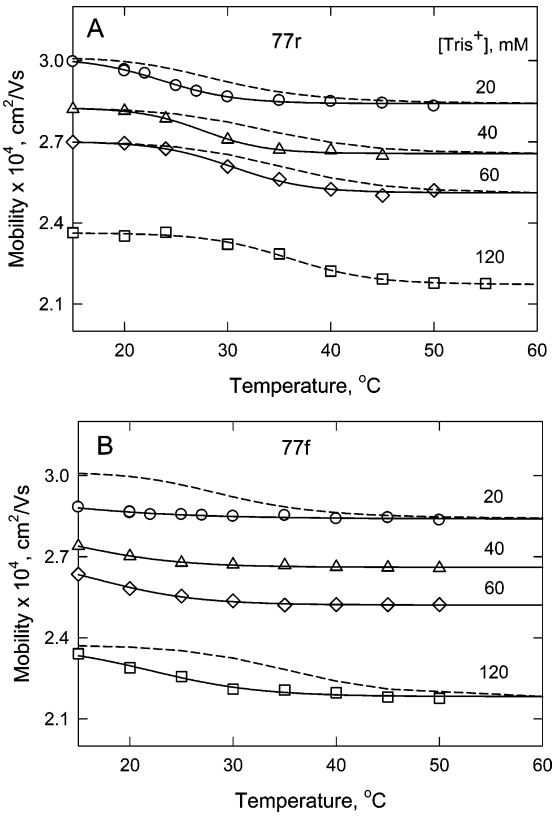

FIGURE 10: Thermal melting curves observed for (A) 77r and (B) 77f, in solutions containing different concentrations of $Tris^+$ ions. In both panels A and B, the symbols represent $Tris^+$ ion concentrations of (○) 20 mM, (△) 40 mM, (◇) 60 mM, and (□) 120 mM. The solid lines were calculated by curve fitting, using the titration spans and melting temperatures given in Table 3. The dashed curves correspond to melting curves calculated from the DINAMelt (*25*) free energies for the most stable hairpin forms of 77r and 77f. The experimental melting curve observed for 77r at 120 mM $Tris^+$ overlaps the predicted melting curve and is not shown for clarity.

Table 3: Comparison of the Melting Temperatures Observed for Oligomers 77r and 77f at Different $Tris^+$ Ion Concentrations with the Melting Temperatures Predicted (*25*) for the Same Oligomers at Comparable Na^+ Ion Concentrations

		77r		77f	
$[M^+]$,[a] mM	$\Delta\mu_{diff}$,[b] mu	obsd T_m in $Tris^+$, °C	predicted T_m in Na^+, °C	obsd T_m in $Tris^+$, °C	predicted T_m in Na^+, °C
20	0.17	24	29	5	31
40	0.17	28	31	14	34
60	0.19	31	33	17	36
120	0.19	36	35	22	38

[a] M^+ is $Tris^+$ or Na^+. [b] Mobility units, 1 mu = 10^{-4} cm^2/Vs; $\Delta\mu_{diff}$ was assumed to be equal for 77r and 77f .

The dependence of the thermal melting temperature of 77r on the logarithm of the $Tris^+$ ion concentration is shown in Figure 11 (open symbols and solid line). The slope of the line, dT_m /d log $[Tris^+]$, is 16.7 °C. A line with a similar slope, but offset on the vertical scale, is obtained for oligomer 77f (not shown). The dependence of the predicted (*25*) melting temperature of 77r on Na^+ ion concentration is shown as the dashed line. The slope of the predicted line is 8.9 °C, similar to the slopes observed for other small DNA hairpins in solutions containing Na^+ ions (*19*, *40*).

The slopes of the lines in Figure 11 can be used to estimate the number of cations released per phosphate residue upon

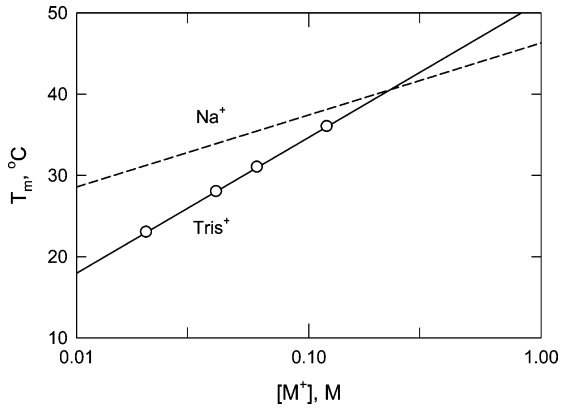

FIGURE 11: Dependence of the melting temperatures, T_m, of 77r on the logarithm of the cation concentration, $[M^+]$, in the solution. The symbols and solid line describe melting temperatures observed in solutions containing various concentrations of $Tris^+$ ions. The dashed line represents T_m values predicted (*25*) for 77r in solutions containing Na^+ ions. The straight lines were calculated by linear regression. The standard errors of the T_m values observed in the $Tris^+$ solutions are smaller than the sizes of the symbols.

denaturation of the hairpin (*17*−*19*, *41*). Cation release occurs because the linear charge density of single-stranded DNA is less than that of double-stranded DNA, so that fewer counterions are condensed around ssDNAs (*42*). For polymeric nucleic acids, the number of cations released per phosphate can be estimated from eq 8

$$\text{slope} = d(T_m)/d \log [M^+] = -2.3(\alpha R T_m^2/\Delta H^\circ)\,\Delta n \quad (8)$$

where R is the gas constant, α is a factor that accounts for changes in the activity coefficient of the cation with concentration and is often set equal to 0.9 (*41*), ΔH° is the enthalpy of melting per nucleotide, and Δn is the number of cations released per nucleotide (*17*, *19*, *40*, *41*). Because end effects do not appear to affect the slopes of such plots (*43*), the same equation can be used to estimate cation release from small DNA hairpins. The factor in parentheses on the right-hand side of eq 8 is not significantly salt- and temperature-dependent (*18*, *19*) and is often given the value of 50 (*19*). Using this value, the number of $Tris^+$ ions released per phosphate upon denaturation of oligomer 77r is estimated to be 0.15. From the dashed line in Figure 11, 0.08 Na^+ ion per phosphate is predicted to be released upon denaturation. Previous studies with hairpins of similar size have found that 0.06−0.12 Na^+ ion is released per phosphate residue (*19*, *40*, *41*).

The results in Figure 11 suggest that more $Tris^+$ ions than Na^+ ions are released upon thermal denaturation of oligomer 77r. Either the hairpin form of this oligomer binds more $Tris^+$ ions than Na^+ ions, so that more $Tris^+$ ions are released upon denaturation, or the random coil form binds fewer $Tris^+$ ions than Na^+ ions. Plots such as those shown in Figure 11 cannot distinguish between these two alternatives (*43*). However, recent studies have shown that duplex DNAs have a higher affinity for $Tris^+$ ions than for Na^+ ions, whereas single-stranded DNAs do not bind either cation significantly (*44*). The combined results suggest that the greater number of $Tris^+$ ions released upon the denaturation of oligomer 77r is due to the fact that DNA hairpins bind more $Tris^+$ ions than Na^+ ions. Hydrogen bonding between the $Tris^+$ ions and the

nucleotide bases may explain the increased binding affinity of $Tris^+$ ions (*44*, *45*).

CONCLUDING REMARKS

The results in this study indicate that the highly variable electrophoretic mobilities observed for single-stranded DNA oligomers in polyacrylamide gels and in free solution are due to differences in the secondary structures of the oligomers, most likely hairpin formation. The mobilities of all tested members of the variable %AT family became equal after chemical (Figure 5B) or thermal (Table 2) denaturation, as expected for oligomers containing the same number of bases. Because DNA hairpins and random coils are in rapid equilibrium (*21*−*23*), the mobility observed for each oligomer under non-denaturing conditions is the weighted average of the mobilities of the various conformational isomers present in the solution.

The actual value of the observed mobility depends on the buffer used for electrophoresis, because the mobility is directly proportional to the intrinsic conductivities of the various ions in the solution (*32*, *39*, *46*) and inversely proportional to the square root of ionic strength (*28*). The average mobility observed for oligomers in the slow mobility group (62f, 62r, and 77f) at 20 °C in 40 mM Tris acetate buffer was 2.87 mu (Table 2). When corrected for differences in the conductivity and ionic strength of Tris acetate and sodium diethylmalonate buffers, the predicted mobility of these oligomers in sodium diethylmalonate buffer is 3.08 mu, very close to the observed mobility, 3.12 mu (Figure 4).

The mobilities observed at 20 °C (column 7 in Table 2) and the limiting mobilities of the hairpin and random coil forms of each oligomer (columns 2 and 3 in Table 2) can be used to estimate the relative population of hairpins in each conformational ensemble. These relative hairpin populations are given in the last column of Table 2. Oligomers in the slow mobility group (62f, 62r, and 77f) have apparent hairpin populations ranging from 0 to 35% at 20 °C; oligomers with intermediate mobilities (42f, 42r, and 77r) have apparent hairpin populations ranging from 71 to 86%; and the oligomers with the highest mobilities (81f and 81r) appear to be nearly completely in the hairpin form at 20 °C.

The experiments described here were focused on the variable %AT family, each member of which contained two phased AAAAT or TTTTA sequence motifs and various nucleotides in the flanking sequences, so that the total A + T content ranged from 38 to 81%. As described above, the observed mobilities are not correlated with nucleotide composition. In addition, the variable electrophoretic mobilities are not dependent on the presence or absence of A or T tracts. Equally variable gel and free solutions mobilities have been observed for 50 other single-stranded oligomers with different sequences and constant A + T ratios (data not shown). Hence, the electrophoretic mobility of a single-stranded DNA oligomer is not necessarily indicative of the number of nucleotides in the sample; the mobility reflects the extent of hairpin formation as well.

The structure prediction algorithm DINAMelt (*25*) assumes that Na^+, K^+, and NH_4^+ ions have equivalent effects on DNA folding (*15*, *16*, *38*). Another study has shown that similar numbers of Li^+, Na^+, K^+, and Cs^+ ions are released upon the thermal denaturation of a small DNA duplex (*47*). However, the results in Figure 11 indicate that all monovalent cations are not equivalent; significantly more $Tris^+$ ions per phosphate are released from DNA hairpins than are predicted (*25*) or observed (*19*) for the release of Na^+ ions. The greater affinity of duplex DNA for $Tris^+$ ions than for Na^+ ions (*44*) may contribute to this result.

The melting temperatures predicted by DINAMelt (*25*) for the various members of the variable %AT family were similar to the observed T_m values for only half of the oligomers (42r, 77r, 81f, and 81r), as shown in Table 2. The measured T_m of oligomer 42f was significantly higher than the predicted value, possibly because this oligomer forms an unusually stable minihairpin near one end. By contrast, the measured T_m values of oligomers 62f, 62r, and 77f were significantly lower than the predicted values, possibly because the algorithm is less accurate at low ionic strengths (*43*). Alternatively, differences in the binding of $Tris^+$ and Na^+ ions at low ionic strengths may affect the hairpin/coil conformational equilibrium. The measured and predicted melting temperatures became more similar with increasing ionic strength, as shown for oligomers 77f and 77r in Table 3, possibly because cation binding approaches saturation at high ionic strengths (*44*), causing the effective charge of the oligomers to become independent of cation identity. Parallel studies of monovalent cation binding to DNA hairpins (and duplexes) and the effect of different cations on hairpin (or duplex) stability are needed to better understand these effects. Such studies are underway in this laboratory.

REFERENCES

1. Blommers, J. J. J., Walters, J. A. L. I., Haasnoot, C. A. G., Aelen, J. M. A., van der Marel, G. A., van Boom, J. H., and Hilbers, C. W. (1989) Effects of base sequence on the loop folding in DNA hairpins, *Biochemistry 28*, 7491−7498.
2. Nakano, M., Moody, E. M., Liang, J., and Bevilacqua, P. C. (2002) Selection for thermodynamically stable DNA tetraloops using temperature gradient gel electrophoresis reveals four motifs: d(cGNNAg), d(cGNABg), d(cCNNGg), and d(gCNNGc), *Biochemistry 41*, 14283−14292.
3. Varani, G. (1995) Exceptionally stable nucleic acid hairpins, *Annu. Rev. Biophys. Biomol. Struct. 24*, 379−404.
4. Bonnet, G., Tyagi, S., Libchaber, A., and Kramer, F. R. (1999) Thermodynamic basis of the enhanced specificity of structured DNA probes, *Proc. Natl. Acad. Sci. U.S.A. 96*, 6171−6176.
5. Goddard, N. L., Bonnet, G., Krichevsky, O., and Libchaber, A. (2000) Sequence dependent rigidity of single stranded DNA, *Phys. Rev. Lett. 85*, 2400−2403.
6. Wallace, M. I., Ying, L., Balasubramanian, S., and Klenerman, D. (2000) FRET fluctuation spectroscopy: exploring the conformational dynamics of a DNA hairpin loop, *J. Phys. Chem. B 104*, 11551−11555.
7. Wallace, M. I., Ying, L., Balasubramanian, S., and Klenerman, D. (2001) Non-Arrhenius kinetics for the loop closure of a DNA hairpin, *Proc. Natl. Acad. Sci. U.S.A. 98*, 5584−5589.
8. Tan, W., Wang, K., and Drake, T. J. (2004) Molecular beacons, *Curr. Opin. Chem. Biol. 8*, 547−553.
9. Hirao, I., Nishimura, Y., Tagawa, Y., Watanabe, K., and Miura, K. (1992) Extraordinarily stable mini-hairpins: electrophoretical and thermal properties of the various sequence variants of d(GCGAAAGC) and their effect on DNA sequencing, *Nucleic Acids Res. 20*, 3891−3896.
10. Yoshizawa, S., Kawai, G., Watanabe, K., Miura, K., and Hirao, I. (1997) GNA trinucleotide loop sequences producing extraordinarily stable DNA minihairpins, *Biochemistry 36*, 4761−4767.
11. Padrta, P., Štefl, R., Králík, L., Žídek, L., and Sklenář, V. (2002) Refinement of d(GCGAAGC) hairpin structure using one- and two-bond residual dipolar couplings, *J. Biomol. NMR 24*, 1−14.
12. Moody, E. M., and Bevilacqua, P. C. (2004) Structural and energetic consequences of expanding a highly cooperative stable DNA hairpin loop, *J. Am. Chem. Soc. 126*, 9570−9577.

13. Williamson, J. R., and Boxer, S. G. (1989) Multinuclear NMR studies of DNA hairpins. 2. Sequence-dependent structural variations, *Biochemistry 28*, 2831−2836.
14. Chou, S.-H., Chin, K.-H., and Wang, A. H.-J. (2003) Unusual DNA duplex and hairpin motifs, *Nucleic Acids Res. 31*, 2461−2474.
15. Zuker, M. (2003) Mfold web server for nucleic acid folding and hybridization prediction, *Nucleic Acids Res. 31*, 3406−3415.
16. SantaLucia, J., Jr. (1998) A unified view of polymer, dumbbell, and oligonucleotide DNA nearest-neighbor thermodynamics, *Proc. Natl. Acad. Sci. U.S.A. 95*, 1460−1465.
17. Record, M. T., Jr., Zhang, W., and Anderson, C. F. (1998) Analysis of effects of salts and uncharged solutes on protein and nucleic acid equilibria and processes: a practical guide to recognizing and interpreting polyelectrolyte effects, Hofmeister effects, and osmotic effects of salts, *Adv. Protein Chem. 51*, 281−353.
18. Bond, J. P., Anderson, C. F., and Record, M. T., Jr. (1994) Conformational transitions of duplex and triplex nucleic acid helices: thermodynamic analysis of effects of salt concentration on stability using preferential interaction coefficients, *Biophys. J. 67*, 825−836.
19. Shkel, I. A., and Record, M. T., Jr. (2004) Effect of the number of nucleic acid oligomer charges on the salt dependence of stability (ΔG_{37}°) and melting temperature (T_m): NLPB analysis of experimental data, *Biochemistry 43*, 7090−7101.
20. Shen, Y., Kuznetsov, S. V., and Ansari, A. (2001) Loop dependence of the dynamics of DNA hairpins, *J. Phys. Chem. B 105*, 12202−12211.
21. Grunwell, J. R., Glass, J. L., Lacoste, T. D., Deniz, A. A., Chemla, D. S., and Schultz, P. G. (2001) Monitoring the conformational fluctuations of DNA hairpins using single-pair fluorescence resonance energy transfer, *J. Am. Chem. Soc. 123*, 4295−4303.
22. Protozanova, E., Yakovchuk, P., and Frank-Kamenetskii, M. D. (2004) Stacked−unstacked equilibrium at the nick site of DNA, *J. Mol. Biol. 342*, 775−785.
23. Stellwagen, E., Renze, A., and Stellwagen, N. C. (2007) Capillary electrophoresis is a sensitive monitor of the hairpin-random coil transition in DNA oligomers, *Anal. Biochem. 365*, 103−110.
24. Viovy, J.-L. (2000) Electrophoresis of DNA and other polyelectrolytes: physical mechanisms, *Rev. Mod. Phys. 72*, 813−872.
25. Markham, N. R., and Zuker, M. (2005) DINAMelt web server for nucleic acid melting prediction, *Nucleic Acids Res. 33*, W577−W581.
26. Holmes, D. L., and Stellwagen, N. C. (1991) Estimation of polyacrylamide gel pore size from Ferguson plots of normal and anomalously migrating DNA fragments I. Gels containing 3% *N*,*N*′-methylenebisacrylamide, *Electrophoresis 12*, 253−263.
27. Dong, Q., Stellwagen, E., Dagle, J. M., and Stellwagen, N. C. (2003) Free solution mobility of small single-stranded oligonucleotides with variable charge densities, *Electrophoresis 24*, 3323−3329.
28. Stellwagen, E., and Stellwagen, N. C. (2007) Quantitative analysis of cation binding to the adenosine nucleotides using the Variable Ionic Strength method: validation of the Debye−Hückel−Onsager theory of electrophoresis in the absence of counterion binding, *Electrophoresis 28*, 1053−1062.
29. Stellwagen, N. C., Gelfi, C., and Righetti, P. G. (1997) The free solution mobility of DNA, *Biopolymers 42*, 687−703.
30. Dawson, R. M. C., Elliott, D. C., Elliott, W. H., and Jones, K. M., Eds. (1969) *Data for Biochemical Research*, 2nd ed., p 481, Clarendon Press, Oxford, U.K.
31. Grossman, P. D. (1992) Factors affecting the performance of capillary electrophoresis separations: Joule heating, electroosmosis, and zone dispersion, in *Capillary Electrophoresis, Theory and Practice* (Grossman, P. D., and Colburn, J. D., Eds.) pp 3−43, Academic Press, San Diego, CA.
32. Manning, G. S. (1981) Limiting laws and counterion condensation in polyelectrolyte solutions. 7. Electrophoretic mobility and conductance, *J. Phys. Chem. 85*, 1506−1515.
33. O'Brien, R. W., and White, L. R. (1978) Electrophoretic mobility of a spherical colloidal particle, *J. Chem. Soc., Faraday Trans. 74*, 1607−1626.
34. Michov, B. M. (1988) Radically simplifying the Henry function, *Electrophoresis 9*, 199−200.
35. Cleland, R. L. (1991) Electrophoretic mobility of wormlike chains: II. Theory, *Macromolecules 24*, 4391−4402.
36. Pitts, W., Tabor, B. E., Daly, J. (1970) Concentration dependence of electrolyte conductance. 2. Comparison of experimental data with the Fuoss−Onsager and Pitts treatments, *Trans. Faraday Soc. 66*, 693−707.
37. Peyret, N. (2000) Prediction of nucleic acid hybridization: parameters and algorithms, Ph.D. dissertation, Wayne State University, Detroit, MI.
38. SantaLucia, J., Jr., and Hicks, D. (2004) The thermodynamics of DNA structural motifs, *Annu. Rev. Biophys. Biomol. Struct. 33*, 415−440.
39. Stellwagen, E., and Stellwagen, N. C. (2003) Probing the electrostatic shielding of DNA with capillary electrophoresis, *Biophys. J. 84*, 1855−1866.
40. Rentzeperis, D., Kharakoz, D. P., and Marky, L. A. (1991) Coupling of sequential transitions in a DNA double hairpin: energetics, ion binding, and hydration, *Biochemistry 30*, 6276−6283.
41. Mandell, K. E., Vallone, P. M., Owczarzy, R., Riccelli, P. V., and Benight, A. S. (2006) Studies of DNA dumbbells. VIII. Melting analysis of DNA dumbbells with dinucleotide repeat stem sequences, *Biopolymers 82*, 199−221.
42. Manning, G. S. (1978) The molecular theory of polyelectrolyte solutions with applications to the electrostatic properties of polynucleotides, *Q. Rev. Biophys. 11*, 179−246.
43. Owczarzy, R., You, Y., Moreira, B. G., Manthey, J. A., Huang, L, Behlke, M. A., and Walder, J. A. (2004) Effects of sodium ions on DNA duplex oligomers: improved predictions of melting temperatures, *Biochemistry 43*, 3537−3554.
44. Stellwagen, E., Dong, Q., and Stellwagen, N. C. (2007) Quantitative analysis of monovalent counterion binding to random-sequence, double-stranded DNA using the Replacement Ion method, *Biochemistry 46*, 2050−2058.
45. Fischer, B. E., Häring, U. K., Tribolet, R., and Sigel, H. (1979) Metal ion/buffer interactions, *Eur. J. Biochem. 94*, 523−530.
46. Stellwagen, E., Dong, Q., and Stellwagen, N. C. (2005) Monovalent cations affect the free solution mobility of DNA by perturbing the hydrogen-bonded structure of water, *Biopolymers 78*, 62−68.
47. Nakano, S., Fujimoto, M., Hara, H., and Sugimoto, N. (1999) Nucleic acid duplex stability: influence of base composition on cation effects, *Nucleic Acids Res. 27*, 2957−2965.

BI701058F